Enhancement of ferromagnetism by decreasing tolerance factor in electron-doped manganites

T. Qian,[1] P. Tong,[1] Bongju Kim,[1] Sung-Ik Lee,[2] Namsoo Shin,[3] S. Park,[4] and Bog G. Kim[1,*]
[1]*Department of Physics and Research Center for Dielectric and Advanced Matter Physics, Pusan National University, Busan 609-735, Korea*
[2]*National Creative Research Initiative Center for Superconductivity, Department of Physics, Pohang University of Science and Technology, Pohang 790-784, Korea*
[3]*Pohang Accelerator Laboratory, Pohang University of Science and Technology, Pohang 790-784, Korea*
[4]*HANARO Center, Korea Atomic Energy Research Institute, Daejeon 305-353, Korea*
(Received 16 August 2007; revised manuscript received 21 February 2008; published 19 March 2008)

We investigate the origin of the anomalous enhancement of ferromagnetism with decreasing the tolerance factor t in $La_{0.15-x}Y_xCa_{0.85}MnO_3$. The decrease of t bends the Mn-O-Mn bond angles from 180°, which weakens the antiferromagnetic (AFM) interaction and leads to the decrease of the monoclinic C-type AFM phase transition temperature, as well as its phase fraction. This change reduces the effect of the shear strain on the Jahn-Teller splitting of MnO_6 octahedra in the residual orthorhombic phase, which favors the development of the Griffiths phase and thereby enhances the ferromagnetism at low temperatures. Our results provide strong evidence that the effect of the coexisting AFM phase is the dominant factor determining the strength of the ferromagnetism of slightly electron-doped manganites.

DOI: 10.1103/PhysRevB.77.094423 PACS number(s): 75.30.Kz, 75.30.Cr, 75.30.Et, 75.47.Lx

It is known that magnetic and electronic properties of perovskite manganites can be changed over a wide range by varying the tolerance factor t.[1] A decrease of t enhances the buckling effect and bends the Mn-O-Mn bond angles θ from 180°, which decreases the effective e_g electron hopping kinetic energy t_{eff}. When t_{eff} becomes sufficiently small, the electrons are strongly localized by the competing electron-phonon interaction. The localization of the electrons is adverse to the ferromagnetic (FM) interaction based on the double-exchange (DE) mechanism. Therefore, the manganites tend to transform from a FM metallic state to an antiferromagnetic (AFM) insulated state with the decrease of t.

This rule is well observed for hole- and half-doped manganites.[2,3] However, it cannot be applied to lightly electron-doped manganites, where the ferromagnetism is dramatically enhanced and an insulator-metal (IM) transition occurs with decreasing t.[4–8] The unusual behavior in the electron-doped manganites was initially observed in $Pr_{0.13-y}Sm_yCa_{0.83}MnO_3$, for which the A-site ionic size mismatch increases with decreasing t.[4] Since a larger A-site disorder may lead to an AFM state collapsing into a FM state or a spin-cluster glass state,[9,10] the enhancement of the ferromagnetism is naturally attributed to the size mismatch effect. However, more researches have exhibited that the ferromagnetism in the electron-doped manganites, such as $Gd_{0.08}(Ca_ySr_{1-y})_{0.92}MnO_3$ and $Sm_{0.1}Ca_{0.9-y}Sr_yMnO_3$,[6,7] is also enhanced with decreasing both t and the size mismatch. In addition, it was found that the Curie-Weiss temperature (Θ) increases slightly and the AFM transition temperature T_N decreases with decreasing t in $Sm_{0.1}Ca_{0.9-y}Sr_yMnO_3$.[7] Up to now it is still unclear that how the variance of t affects the competing FM and AFM interactions in the paramagnetic (PM) state in the electron-doped manganites and how the effect causes the unusual behavior of the ferromagnetism at low temperatures.

In this paper we found that in the electron-doped manganites $La_{0.15-x}Y_xCa_{0.85}MnO_3$, the monoclinic C-type AFM (C-AFM) phase transition temperature $T_N(C)$ gradually decreases with increasing x, i.e., decreasing t, and is proportional to $\langle\cos^2\theta\rangle$, which is described under the semicovalent-exchange mechanism. Concomitantly, Θ slightly increases with increasing x, which suggests that the FM interaction in the PM state is more strongly affected by the competing AFM interaction rather than the electron bandwidth. Interestingly, for $0\leq x\leq 0.125$ the residual orthorhombic phase is distorted below $T_N(C)$, arising from the shear strain because of the lattice mismatch between the monoclinic and orthorhombic phases. The distortion increases the Jahn-Teller (JT) splitting of MnO_6 octahedra and thereby strongly suppresses the FM interactions. The effect of the shear strain is reduced with increasing x and vanishes at $x=0.15$, which favors the development of the Griffiths phase and finally leads to the enhancement of the ferromagnetism at low temperatures.

Ceramic samples of $La_{0.15-x}Y_xCa_{0.85}MnO_3$ with $0\leq x\leq 0.15$ were synthesized by a standard solid state reaction method and finally sintered at 1300 °C for 24 h. Magnetization (M) was measured using a superconducting quantum interference device magnetometer. Resistivity (ρ) was measured using a standard four-probe technique. Synchrotron x-ray power diffraction (SXRPD) patterns at 300 K were collected on the high resolution powder diffraction beamline 8C2 ($\lambda=1.5496$ Å) of the Pohang Accelerator Laboratory (Pohang, Korea). Normal power x-ray diffraction (XRD) patterns between 80 K and 300 K were recorded by a Bruker D8 Advance diffractometer with a Lynxeye detector using Cu $K\alpha$ radiation. Neutron powder diffraction (NPD) patterns for $x=0$ and 0.15 were collected at various temperatures at the Hanaro Neutron Diffraction Facility (Daejeon, Korea). The SXRPD, XRD and NPD data were analyzed by Rietveld refinement using the FULLPROF program.

Figure 1 shows the M (T) curves measured on warming at magnetic field $H=1$ mT after field-cooling for $La_{0.15-x}Y_xCa_{0.85}MnO_3$ with $0\leq x\leq 0.15$. For all samples below 100 K the magnetization increases rapidly with decreasing temperature, implying an appearance of FM components. Interestingly, the magnetization at low temperatures in-

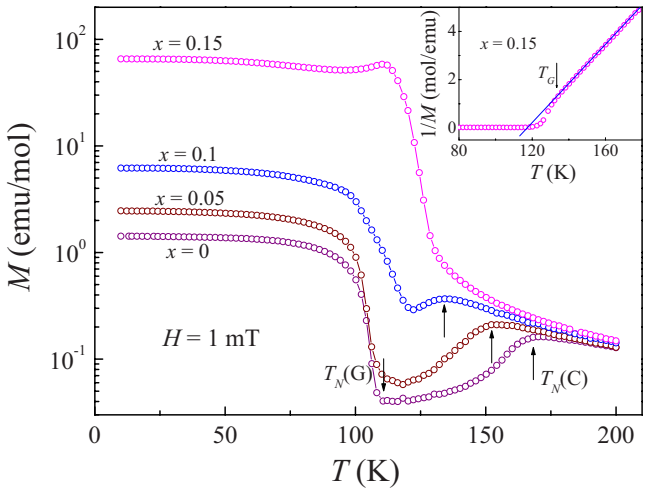

FIG. 1. (Color online) M (T) curves measured at $H=1$ mT for $x=0$, 0.05, 0.1, and 0.15. Inset: Inverse magnetization $1/M(T)$ for $x=0.15$. The solid line indicates a Curie-Weiss behavior. The C-AFM phase transition temperature $T_N(C)$, the G-AFM phase transition temperature $T_N(G)$, and the characteristic temperature T_G of the onset of Griffiths phase are indicated.

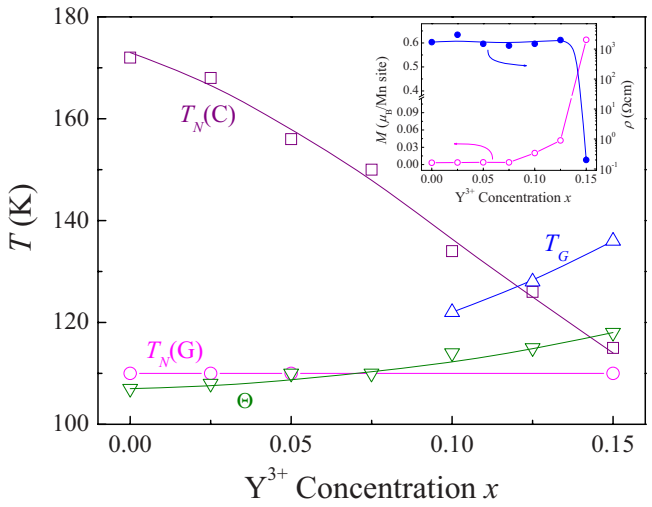

FIG. 2. (Color online) Phase diagram of the $La_{0.15-x}Y_xCa_{0.85}MnO_3$ series with $0\leq x\leq 0.15$. $T_N(C)$ for $x=0.125$ and 0.15 is determined from M (T) curves under $H=5$ T as the rapid increase of the low-field magnetization covers up the C-AFM transitions of the two samples. The Curie-Weiss temperature Θ is determined from inverse susceptibility curves in the temperature range between 200 and 400 K. The definitions of other transition temperatures can be found in the text. Inset: ρ at 20 K and $M_{0\ \mathrm{T}}$ at 10 K as a function of x. $M_{0\ \mathrm{T}}$ is determined by the linear extrapolation of high-field part of M (H) curves at 10 K to $H=0$ T.

creases obviously with increasing x, which indicates the ferromagnetism is enhanced with decreasing t. To understand the unusual behavior, the origin of the FM components needs to be clarified. For $x=0$ the peak around 170 K corresponds to a C-AFM phase transition, which is accompanied by an orthorhombic to monoclinic structural phase transition.[11,12] According to the phase diagram of electron-doped $(La,Ca)MnO_3$, a G-type AFM (G-AFM) spin ordering develops in the residual orthorhombic phase at 110 K.[12] Simultaneously FM polarons form due to doped e_g electrons hopping in the G-AFM phase,[12,13] leading to a sharp increase of the magnetization at 110 K. As x is increased to 0.05, T_N(C) moves toward lower temperatures while the G-AFM phase transition temperature T_N(G), at which the magnetization increases sharply, persists at 110 K. Our NPD data exhibit that the G-AFM phase transitions of the $x=0$ and 0.15 samples occur at about 110 K, implying that T_N(G) is independent on x. However, it is found that for $x\geq 0.1$ the magnetization starts to increase rapidly above 120 K. As shown in the inset of Fig. 1, the inverse susceptibility $1/M$(T) for $x=0.15$ exhibits a deviation from the Curie-Weiss behavior at 136 K. This downtown behavior is characteristic of the Griffiths singularity, corresponding to the appearance of FM clusters in the paramagnetic (PM) phase below the characteristic temperature T_G.[14–19] Moreover, from the linear fitting of the high-temperature $1/M$(T), the effective magnetic moment μ_{eff} is estimated as $4.95\mu_B$/Mn, which is larger than its theoretical counterpart $(4.05\mu_B/\mathrm{Mn})$, indicating the trace of FM clusters with larger magnetic moments than the individual magnetic ions.[18] Therefore, the rapid increase of the magnetization above $T_N(G)$ for $x\geq 0.1$ arises from the growth of FM clusters in the PM phase.

These magnetization data are summarized in the magnetic phase diagram in Fig. 2. In addition, the x dependence of ρ at 20 K and the spontaneous magnetization $M_{0\ \mathrm{T}}$ at 10 K are plotted in the inset of Fig. 2. For $0\leq x\leq 0.075$ $M_{0\ \mathrm{T}}$ is from the FM polarons in the G-AFM phase and hardly changeable with x. With further increasing x, $M_{0\ \mathrm{T}}$ starts to increase obviously while the Griffiths phase appears, which means that the enhancement of the ferromagnetism is associated with the FM clusters appearing in the PM phase. Moreover, $T_N(C)$ decreases gradually with increasing x. It is noticed that when T_G is beyond $T_N(C)$ at x close to 0.15, $M_{0\ \mathrm{T}}$ exhibits a sharp increase, which is accompanied by an IM transition. These results suggest that the strength of the ferromagnetism is strongly affected by the C-AFM phase. Therefore, it is important to reveal the relationship between t and the C-AFM phase.

The t dependence of $T_N(C)$ in Fig. 2 is similar to those in the single-valent $Ca_{1-x}Sr_xMnO_3$ and $RMnO_3$ (R=La, Pr, Nd, and Sm) systems, which has been explained under the semicovalent-exchange mechanism.[20,21] According to the semicovalent-exchange theory, the change of T_N relates primarily to the deviation of θ from 180°, which gives a linear relationship between T_N and $\langle\cos^2\theta\rangle$ $(=[\cos^2\theta_1+2\cos^2\theta_2]/3)$. Here, θ_1 and θ_2 represent θ along the b axis and in the ac place, namely Mn-O_1-Mn and Mn-O_2-Mn bond angles,[20] respectively. In order to obtain structural information, we carried out Rietveld refinements based on the SXRPD data at 300 K with the space group *Pnma*. Figure 3(a) shows the evolution of the lattice parameters at 300 K with x. The a axis is less changed while the b and c axes are obviously decreased with increasing x, indicating the increase of lattice distortion. Since the concentration of Mn^{3+} ions is fixed in the $La_{0.15-x}Y_xCa_{0.85}MnO_3$ series, the increasing lattice distortion arises from the enhanced

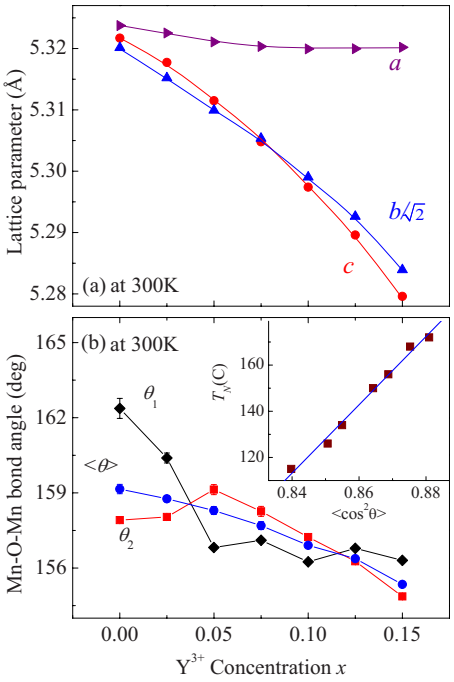

FIG. 3. (Color online) (a) Lattice parameters and (b) bond angles for $La_{0.15-x}Y_xCa_{0.85}MnO_3$ as a function of x at 300 K.

buckling effect due to the smaller radius of Y^{3+} ions rather than the JT effect.[22] Moreover, the structural transformation from an O′- $(a>c>b/\sqrt{2})$ to O-type $(a>b/\sqrt{2}>c)$ orthorhombic symmetry around $x=0.075$ is a consequence of the buckling effect.[23] Under the buckling effect MnO_6 octahedra are gradually tilted with decreasing t, leading to the deviation of θ from 180°.[6,24] The refined bond angles, θ_1, θ_2 and their average $\langle\theta\rangle$ are plotted in Fig. 3(b), from which the value of $\langle\cos^2\theta\rangle$ can be estimated. As seen in the inset of Fig. 3(b), $T_N(C)$ shows a linear relationship with $\langle\cos^2\theta\rangle$, in accordance with the semicovalent-exchange mechanism. This provides strong evidence that the decrease of $T_N(C)$ arises from the reduced σ-bonding overlap integral due to the tilting of MnO_6 octahedra.[21]

From a viewpoint of DE, the tilting of MnO_6 octahedra also disfavors the FM interaction in manganites. However, since in our system the concentration of Mn^{3+} ions is fairly low, the AFM interaction between Mn^{4+} ions remains dominant. Therefore, the FM interaction is also strongly affected by the competitive AFM interaction, which is weakened with the decrease of t. In Fig. 2 Θ increases lightly with increasing x. For other electron-doped manganites, Θ exhibits similar t dependence.[7] These results suggest that the direct effect of the electron bandwidth on the FM interaction is a minor scenario in slightly electron-doped manganites, whereas the AFM interaction plays a more important role in determining the strength of the FM interaction.

However, as compared with the slight increase of Θ, $M_{0\ T}$ exhibits complex and strong dependence on x. In particular, $M_{0\ T}$ increases sharply at x close to 0.15. The evolution of the ferromagnetism at low temperatures with x cannot be explained by the strength of the FM coupling at high temperatures. It should be mentioned that the ferromagnetism is

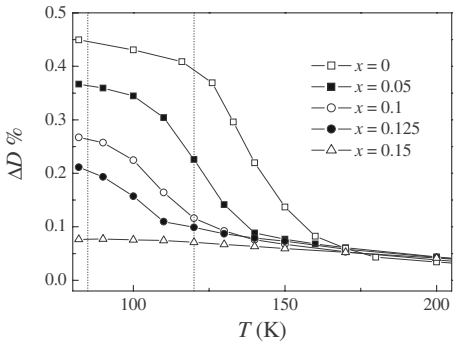

FIG. 4. Temperature dependence of the lattice distortion index $\Delta D\%$ of the orthorhombic phase (deduced from normal powder XRD). The vertical dash lines are plotted at 85 and 120 K for the convenience of comparing the evolution of lattice distortions with temperature and doping.

developed in the orthorhombic phase as the monoclinic phase only includes the C-AFM spin ordering.[12] From the results of Rietveld refinements of the XRD and NPD data at various temperatures, it is found that for $0\leq x\leq 0.125$ the a and c axes of the residual orthorhombic phase are elongated and the b axis is compressed below $T_N(C)$, whereas for $x=0.15$ there is not any anomaly in the lattice parameters of the orthorhombic phase across $T_N(C)$. Therefore, the strength of the ferromagnetism is related to the lattice distortion of the orthorhombic phase below $T_N(C)$. The lattice anomaly occurring at $T_N(C)$ exhibits a relationship between the lattice distortion and the monoclinic C-AFM phase. As compared with those of the original orthorhombic phase, the monoclinic phase has longer a and c axes and a shorter b axis, due to e_g electrons occupying the $d_{3z^2-r^2}$ orbitals in the ac plane.[12] So the increasing lattice distortion of the orthorhombic phase is induced by the shear strain because of the lattice mismatch between the orthorhombic and monoclinic phases, which is similar to that in manganite films.[25] Such a lattice distortion increases the JT splitting and thereby promotes the localization of e_g electrons, which strongly suppresses the FM interaction.[1,26]

In manganites the lattice distortion index D is given by $D=\Sigma|a_i-a|/3a$ [where $a_1=a$, $a_2=b/\sqrt{2}$, $a_3=c$, and $a=(a\times b\times c/\sqrt{2})^{1/3}$].[27] Based on the normal XRD data, the reduced lattice distortion $\Delta D(T)$ $[=D(T)-D(300\ \mathrm{K})]$ of the orthorhombic phase is plotted in Fig. 4. Generally the lattice distortion is related to two factors, i.e., the buckling effect and the JT effect.[1] The high resolution NPD data for the samples with $x=0$ and 0.15 were employed to investigate the details of these two factors. Figure 5 typically shows the refinement of patterns at 90 K. The monoclinic and orthorhombic phases, as well as the corresponding C-AFM and G-AFM phases, respectively, were included in the refinements. Besides, an orthorhombic FM phase, which is absent in $x=0$, should be taken into account for $x=0.15$. The monoclinic fraction is found to decrease from 84.94% for $x=0$ to 57.1% for $x=0.15$ at 90 K. This suggests that the ferromagnetism in the present system is strongly influenced by the coexisting C-AFM monoclinic phase, consistent with the result of the magnetization measurement discussed above (Fig.

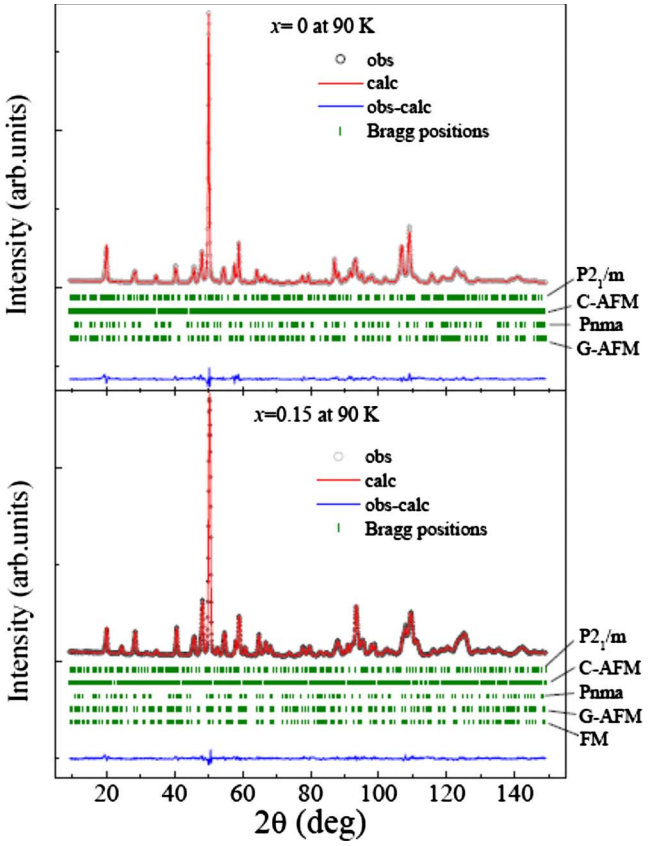

FIG. 5. (Color online) Rietveld refinements of neutron diffraction data at 90 K for $x=0$ and 0.15 using the Fullprof program. The observed (obs), calculated (calc) patterns and the difference between them (obs-calc) are plotted. The vertical bars show the Bragg peak positions.

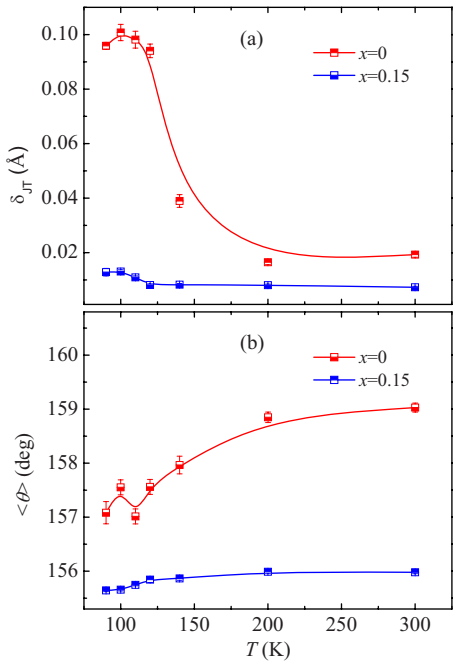

FIG. 6. (Color online) (a) Temperature dependent JT distortion and (b) average Mn-O-Mn bond angle $\langle\theta\rangle$ (b) for the orthorhombic phase in $La_{0.15-x}Y_xCa_{0.85}MnO_3$ with $x=0$ and 0.15. Solid lines are guidance for eyes.

2). The magnitude of JT distortion in orthorhombic phase can be estimated by $\delta_{JT}=\sqrt{\frac{1}{3}\Sigma_i[(\text{Mn-O})_i-\langle\text{Mn-O}\rangle]^2}$, where $(\text{Mn-O})_i$ and $\langle\text{Mn-O}\rangle$ represent the ith bond length of a MnO_6 octahedron and the average bond length, respectively.[28] According to the bond length obtained by the refinement of NPD data, the temperature dependences of δ_{JT} is displayed in Fig. 6(a). At low temperatures δ_{JT} is enhanced significantly for $x=0$, while slightly increased for $x=0.15$. This trend is similar to that of ΔD (T) in Fig. 4. While at room temperature, JT distortion is weak in both samples. On the other hand, as displayed by Fig. 6(b), the average bond angle $\langle\theta\rangle$ (the buckling of MnO_6 octahedra) is less temperature-dependent than δ_{JT}. Furthermore, as proved by Fig. 3, the buckling of MnO_6 octahedra accounts for the lattice distortion at 300 K, $D(300\ \text{K})$. Thus the increase of $\Delta D(T)$ at low temperatures is associated with the JT effect since the contribution from buckling effect is deducted. As a result, with increasing Y^{3+} concentration, the monoclinic fraction decreases, so does the shear strain effect on the residual orthorhombic phase. This change will induce a reduction of lattice (JT) distortion in the orthorhombic phase, favoring the DE ferromagnetism.

Based on the dependences of lattice distortion on temperature and Y^{3+} concentration, the various low-temperature magnetic behaviors can be readily understood. Figure 4 shows three different situations at 85 and 120 K slightly higher than Θ, which correspond to three kinds of behavior in Fig. 1 and Fig. 2, respectively. (1) For $x=0$ and 0.05, ΔD starts to increase at temperature much higher than Θ and reaches a larger value at 120 K, where the large JT splitting completely suppresses the FM interaction. Therefore, the samples with $0\leq x\leq 0.75$ do not exhibit any FM characteristic above $T_N(G)$. The weak ferromagnetism at low temperatures only comes from the FM polarons in the G-AFM phase. (2) For $x=0.1$ and 0.125 ΔD, i.e., the JT splitting, is not very large at 120 K and thereby the Griffiths phase appears above Θ. But with further decreasing temperature, the increase of the JT splitting prevents the Griffiths phase from further growing. Therefore, $M_{0\ \text{T}}$ at 10 K obviously increases but still persists in fairly low values. (3) For $x=0.15$ the Griffiths phase can successfully evolve into a long-range FM state since Θ becomes even higher than $T_N(G)$. The preexistent FM phase partially prevents the growth of the monoclinic phase, which becomes a minor phase at low temperatures. The shear strain is not large enough to distort the orthorhombic phase. As a result, the development of the long-range FM spin ordering leads to the sharp increase of $M_{0\ \text{T}}$ as well as the IM transition, as seen in the inset of Fig. 2.

In conclusion, the ferromagnetism at low temperatures in $La_{0.15-x}Y_xCa_{0.85}MnO_3$ strongly depends on the evolution process of the JT splitting in the orthorhombic phase, which arises from the shear strain because of the lattice mismatch between the orthorhombic and monoclinic C-AFM phases. Moreover, the strength of the FM interaction at high temperatures is more sensitive to the AFM interaction. These results suggest that the coexisting AFM phase as well as the competing AFM interaction plays key roles in determining

the magnetic properties of slightly electron-doped manganites.

We thank Sang-Wook Cheong for helpful discussions. We acknowledge the support from National Core Research Center Program of Pusan National University [R15-2006-02-01002-0(2007)] and by Grant No. R01-2005-000-10354-0 from the Basic Research Program of the Korea Science & Engineering Foundation and by a Korea Research Foundation Grant (KRF-2006-005-J02803). The authors also acknowledge the support from Pohang Light Source and Hanaro neutron facility.

*Corresponding author. boggikim@pusan.ac.kr

[1] A. J. Millis, Nature (London) **392**, 147 (1998).
[2] R. Kajimoto, H. Yoshizawa, Y. Tomioka, and Y. Tokura, Phys. Rev. B **66**, 180402(R) (2002).
[3] H. Y. Hwang, S-W. Cheong, P. G. Radaelli, M. Marezio, and B. Batlogg, Phys. Rev. Lett. **75**, 914 (1995).
[4] A. Maignan, C. Martin, F. Damay, and B. Ravean, Chem. Mater. **10**, 950 (1998).
[5] L. Sudheendra, A. R. Raju, and C. N. R. Rao, J. Phys.: Condens. Matter **15**, 895 (2003).
[6] S. Hirano, J. Sugiyama, T. Noritake, and T. Tani, Phys. Rev. B **70**, 094419 (2004).
[7] V. Markovich, I. Fita, R. Puzniak, C. Martin, A. Wisniewski, S. Hébert, A. Maignan, and G. Gorodetsky, J. Phys.: Condens. Matter **18**, 9201 (2006).
[8] M. Miclau, S. Hébert, R. Retoux, and C. Martin, J. Solid State Chem. **178**, 1104 (2005).
[9] Y. Tomioka and Y. Tokura, Phys. Rev. B **70**, 014432 (2004).
[10] K. F. Wang, F. Yuan, S. Dong, D. Li, and Z. D. Zhang, Appl. Phys. Lett. **89**, 222505 (2006).
[11] M. Pissas, G. Kallias, M. Hofmann, and D. M. Többens, Phys. Rev. B **65**, 064413 (2002).
[12] C. D. Ling, E. Granado, J. J. Neumeier, J. W. Lynn, and D. N. Argyriou, Phys. Rev. B **68**, 134439 (2003).
[13] J. J. Neumeier and J. L. Cohn, Phys. Rev. B **61**, 14319 (2000).
[14] R. B. Griffiths, Phys. Rev. Lett. **23**, 17 (1969).
[15] M. B. Salamon, P. Lin, and S. H. Chun, Phys. Rev. Lett. **88**, 197203 (2002).
[16] J. Deisenhofer, D. Braak, H.-A. Krug von Nidda, J. Hemberger, R. M. Eremina, V. A. Ivanshin, A. M. Balbashov, G. Jug, A. Loidl, T. Kimura, and Y. Tokura, Phys. Rev. Lett. **95**, 257202 (2005).
[17] M. B. Salamon and S. H. Chun, Phys. Rev. B **68**, 014411 (2003).
[18] K. F. Wang, Y. Wang, L. F. Wang, S. Dong, D. Li, Z. D. Zhang, H. Yu, Q. C. Li, and J. M. Liu, Phys. Rev. B **73**, 134411 (2006).
[19] R. F. Yang, Y. Sun, W. He, Q. A. Li, and Z. H. Cheng, Appl. Phys. Lett. **90**, 032502 (2007).
[20] O. Chmaissem, B. Dabrowski, S. Kolesnik, J. Mais, D. E. Brown, R. Kruk, P. Prior, B. Pyles, and J. D. Jorgensen, Phys. Rev. B **64**, 134412 (2001).
[21] J. S. Zhou and J. B. Goodenough, Phys. Rev. B **68**, 054403 (2003).
[22] The results of Rietveld refinements also exhibit that the individual Mn-O bond lengths, which reflect the magnitude of the JT distortion, are insensitive to x.
[23] E. Pollert, S. Krupička, and E. Kuzmičová, J. Phys. Chem. Solids **43**, 1137 (1982).
[24] J. S. Zhou and J. B. Goodenough, Phys. Rev. Lett. **96**, 247202 (2006).
[25] G. Y. Gao, S. W. Jin, and W. B. Wu, Appl. Phys. Lett. **90**, 012509 (2007).
[26] A. J. Millis, T. Darling, and A. Migliori, J. Appl. Phys. **83**, 1588 (1998).
[27] A. Arulraj, P. N. Santhosh, R. Srinivasa Gopalan, A. Guha, A. K. Raychaudhuri, N. Kumar, and C. N. R. Rao, J. Phys.: Condens. Matter **10**, 8497 (1998).
[28] P. G. Radaelli, G. Iannone, M. Marezio, H. Y. Hwang, S-W. Cheong, J. D. Jorgensen, and D. N. Argyriou, Phys. Rev. B **56**, 8265 (1997).